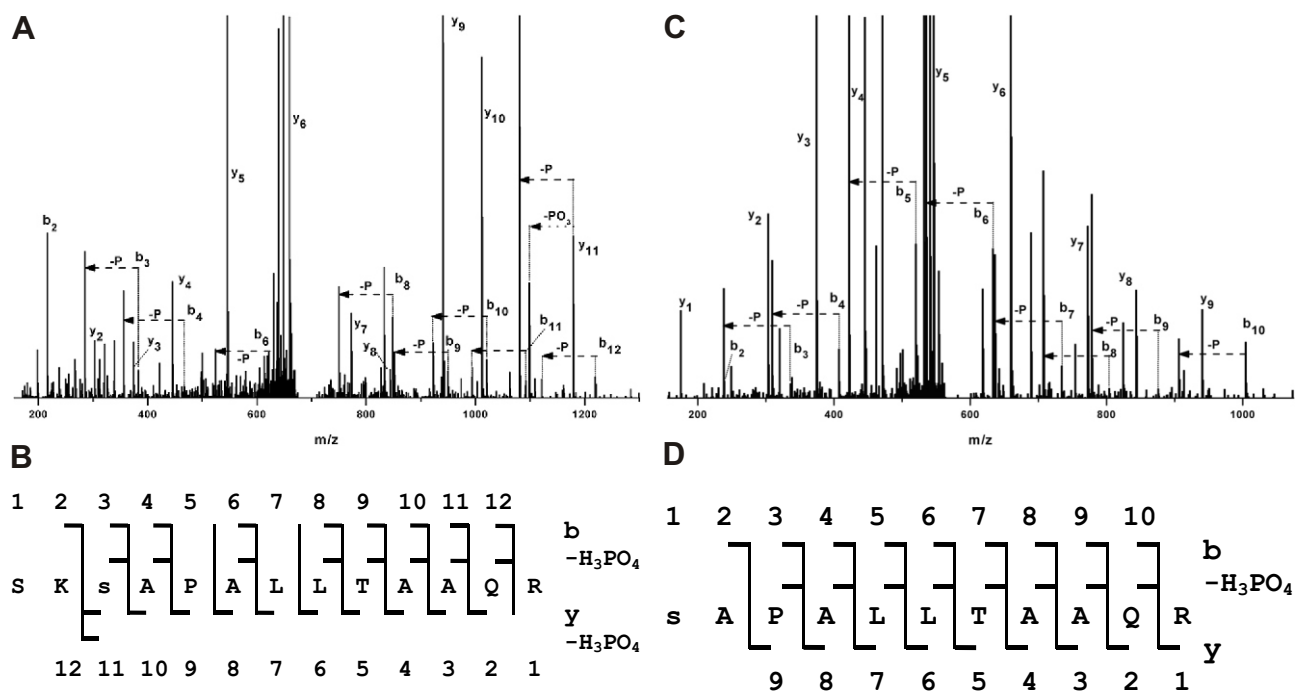
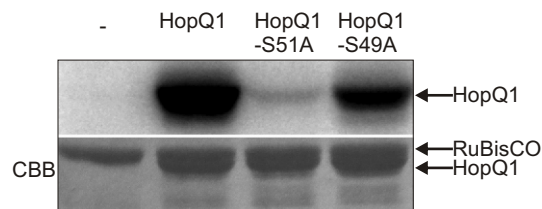


14-3-3 binding motif					RS/T	X	S	X	P							
<i>P.syringae</i> pv. <i>phaseolicola</i> 1448A	44	P	V	L	E	R	S	K	S	A	P	A	L	L	T	A <sub>58</sub>
<i>P.syringae</i> pv. <i>tomato</i> DC3000	44	P	V	L	E	R	S	K	S	A	P	A	L	L	T	A <sub>58</sub>
<i>X.campestris</i> pv. <i>campestris</i> ATCC33913	47	A	V	L	K	R	S	L	S	A	P	A	L	T	A	T <sub>61</sub>
<i>X.campestris</i> pv. <i>vesicatoria</i> 85-10	58	P	R	H	R	R	A	Q	S	L	P	A	R	L	T	P <sub>72</sub>
<i>X.oryzae</i> pv. <i>oryzae</i> KACC10331	83	P	R	H	R	R	T	Q	S	L	P	A	R	L	T	P <sub>99</sub>

14-3-3 binding motif					RS/T	X	S	X	P							
<i>P.syringae</i> pv. <i>phaseolicola</i> 1448A	44	P	V	L	E	R	S	K	S	A	P	A	L	L	T	A <sub>58</sub>
<i>P.syringae</i> pv. <i>tomato</i> DC3000	44	P	V	L	E	R	S	K	S	A	P	A	L	L	T	A <sub>58</sub>
<i>X.campestris</i> pv. <i>campestris</i> ATCC33913	47	A	V	L	K	R	S	L	S	A	P	A	L	T	A	T <sub>61</sub>
<i>X.campestris</i> pv. <i>vesicatoria</i> 85-10	58	P	R	H	R	R	A	Q	S	L	P	A	R	L	T	P <sub>72</sub>
<i>X.oryzae</i> pv. <i>oryzae</i> KACC10331	83	P	R	H	R	R	T	Q	S	L	P	A	R	L	T	P <sub>99</sub>



**Figure 2.** The predicted 14-3-3 binding motif of HopQ1 is phosphorylated by plant kinases. (A, B) HopQ1-Strep-tag II fusion protein expressed in *N. benthamiana* leaves was affinity-purified and subjected to LC-MS-MS/MS analysis. (C, D) HopQ1-6xHis expressed in bacteria was incubated with total protein extracts from *N. benthamiana* and then affinity-purified and analyzed by LC-MS-MS/MS. Panels A and C show the fragmentation spectra with peak assignment to b, y, b-H<sub>3</sub>PO<sub>4</sub> and y-H<sub>3</sub>PO<sub>4</sub>, with “P” denoting loss of a H<sub>3</sub>PO<sub>4</sub> group. Major signals of the MS/MS spectra are identified by their corresponding fragment tags of the b, y series, but also of the y-H<sub>3</sub>PO<sub>4</sub> and b-H<sub>3</sub>PO<sub>4</sub> series, which were expected in the case of a phosphorylated peptide. Panels B and D show the peptide sequences with daughter ions of the b, y, b-H<sub>3</sub>PO<sub>4</sub> and y-H<sub>3</sub>PO<sub>4</sub> series found in the spectra. In the peptide derived from HopQ1 phosphorylated *in vitro* (C, D), the presence of the full series of b2-b10 fragments and the expected b-H<sub>3</sub>PO<sub>4</sub> series allows for unequivocal localization of the phosphate at Ser 51. In the peptide derived from HopQ1 expressed *in planta* (A, B), the majority of b and b-H<sub>3</sub>PO<sub>4</sub> pairs are also present. In addition, the presence of strong y, y-PO<sub>3</sub> and y-H<sub>3</sub>PO<sub>4</sub> signals indicate that the site of phosphorylation is S51 and not S49.



**Figure 3.** Serine 51 plays a critical role in the phosphorylation of HopQ1. Recombinant HopQ1 variants with a C-terminal 6xHis epitope were incubated with leaf protein extracts from *N. benthamiana* in buffer containing [ $\gamma$ <sup>32</sup>P]ATP. Samples were resolved by SDS-PAGE and analyzed by autoradiography. Only residual phosphorylation was detected for HopQ1 mutated at position 51. As a loading control the Coomassie Brilliant Blue (CBB) stained gel is shown in lower panel. The experiment was performed three times with similar results.

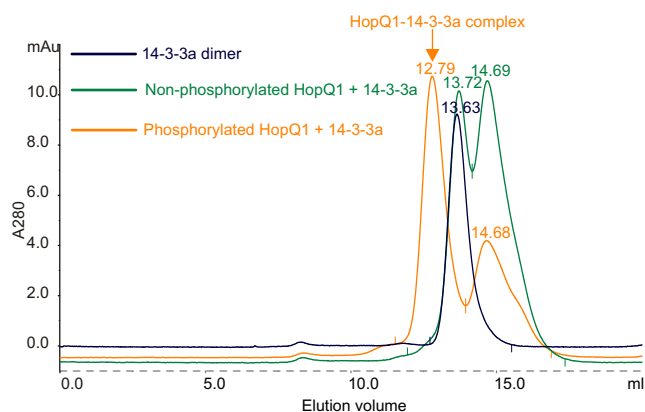


**Figure 4.** HopQ1 binds to 14-3-3a in phosphorylation dependent manner. Representative gel filtration runs on a Superdex 200 column. Recombinant HopQ1 with a C-terminal 6xHis epitope was incubated with recombinant CPK3 prior binding to 14-3-3a (orange trace). As a control non-phosphorylated HopQ1 was used (green trace). Under conditions used (5mM DTT) HopQ1 exists as a monomer (elution volumes 14.68, 14.69). 14-3-3a was eluted as dimers (peaks 13.63, 13.72). Recombinant CPK3 was removed from the reaction by affinity capture on GST-column. The experiment was performed twice with similar results.

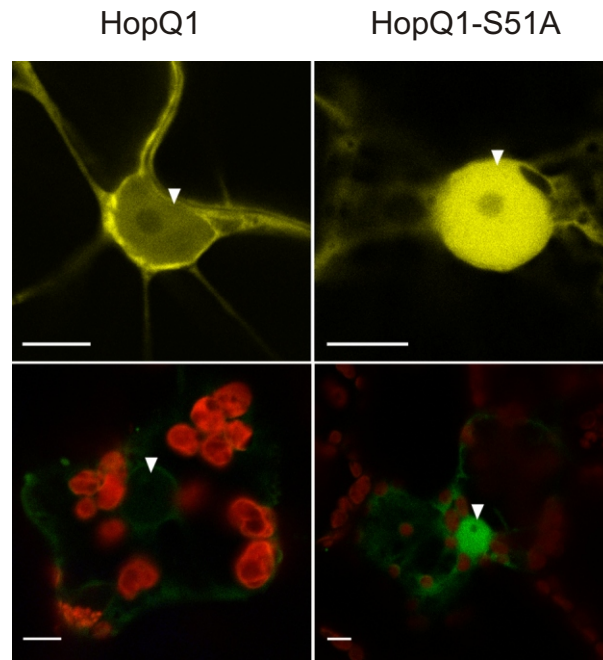


**Figure 5.** Subcellular localization of HopQ1 variants. Confocal images of representative *N. benthamiana* leaf epidermal cells (upper panel) or mesophyll cells (lower panel) transiently expressing either wild-type HopQ1-eYFP (left panel) or HopQ1-S51A-eYFP (right panel). White arrowheads indicate the nuclei. Scale bars represent 10  $\mu\text{m}$ . The pictures were taken 72 h after agroinfiltration. For each variant ca. 50 transformed cells were examined.

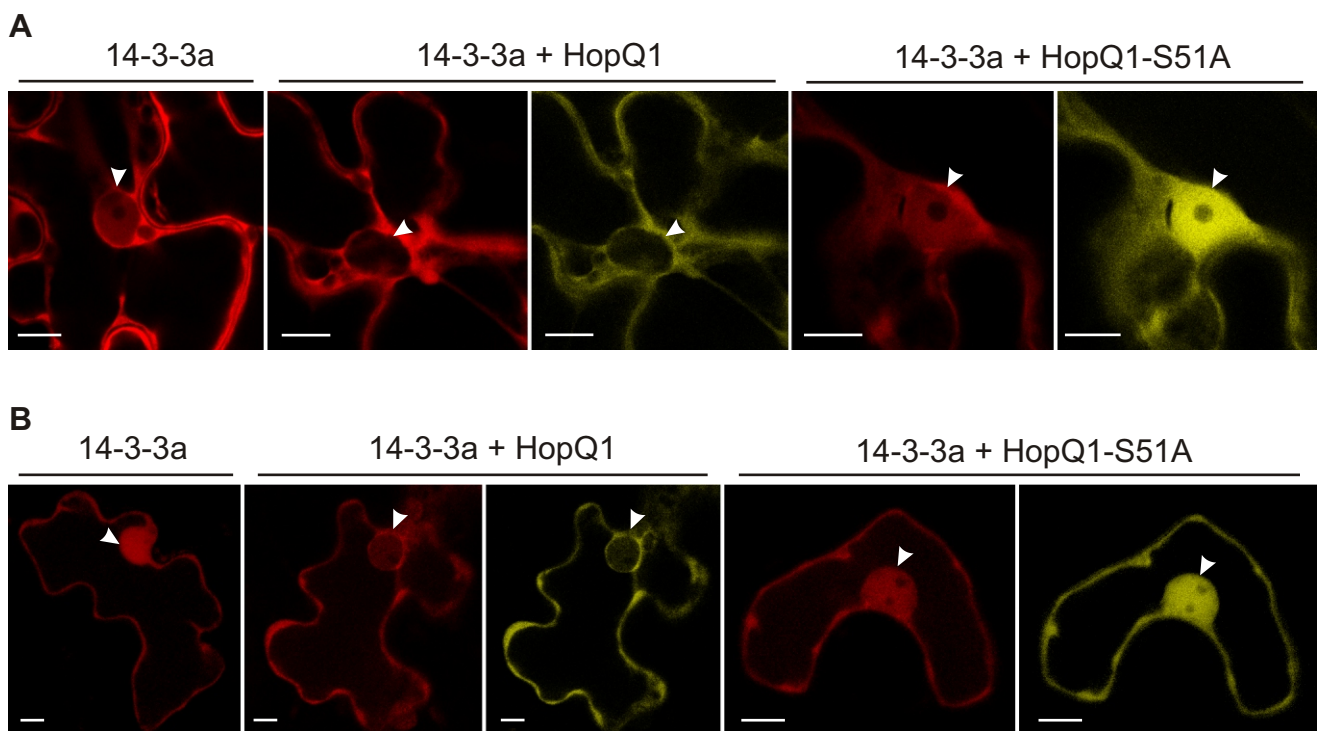


**Figure 6.** Co-expression of 14-3-3a and HopQ1 affects nuclear-cytoplasmic partitioning of the binding partners. (A) *N. benthamiana* leaves were co-infiltrated with *A. tumefaciens* strains carrying constructs encoding 14-3-3a-mRFP and variants of HopQ1 fused to eYFP. For each variant ca. 50 transformed cells were examined. (B) The same constructs were transiently co-expressed in *P. vulgaris* epidermal cells *via* particle bombardment. In both plant species, 14-3-3a-mRFP localized to the cytoplasm and nucleus. Co-expression with wild-type HopQ1-eYFP resulted in the relocation of 14-3-3a-mRFP from the nucleus to the cytoplasm. A non-interacting form of HopQ1 (HopQ1-S51A-eYFP) shows highly increased nuclear accumulation and does not alter the localization of 14-3-3a-mRFP. For each variant ca. 20 transformed cells were examined. White arrowheads indicate the nuclei. Scale bars represent 10  $\mu$ m.

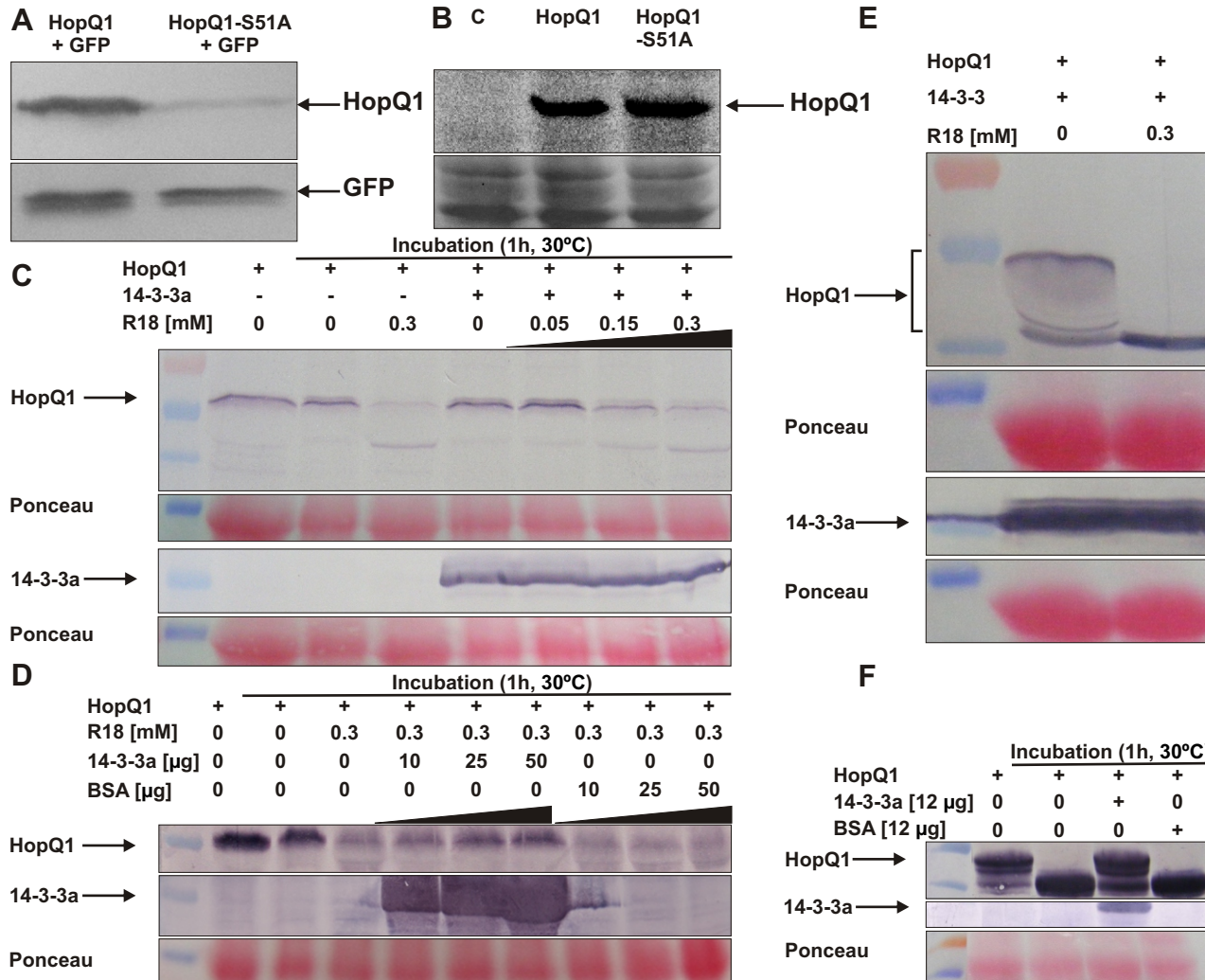


**Figure 7.** The presence of Serine 51 affects HopQ1 stability *in planta*. (A) Wild-type HopQ1 or HopQ1-S51A proteins carrying C-terminal 3xHA epitopes were transiently co-expressed with GFP in *N. benthamiana* leaves. Crude protein extracts (20 μg proteins per lane) were isolated from leaves 48h after agroinfiltration. HopQ1 variants were detected by immunoblot analysis using an antibody specific to HA. As an expression control the level of GFP was checked using anti-GFP antibody. The experiment was repeated twice. (B) C-terminally His-tagged HopQ1 variants were expressed in *P. syringae* pv. *tabaci* DAPP-PG677. Crude protein extracts prepared from overnight bacterial cultures were fractionated on a 12.5% SDS-PAGE and subjected to immunoblot analysis using a specific anti-His antibody. Equal protein loading was shown by Ponceau Red staining. The experiment was repeated twice. (C) R18, the inhibitor of 14-3-3 binding affects HopQ1 stability in plant extracts. Wild-type HopQ1 protein carrying a C-terminal Flag epitope was transiently expressed in *N. benthamiana* leaves. Crude protein extract was supplemented with recombinant 14-3-3-Strep II protein isolated from *E. coli* or R18 peptide at various concentrations, as indicated. HopQ1 and 14-3-3a were detected by immunoblot analysis using specific primary antibody. Equal protein loading was shown by Ponceau Red staining. (D) Application of 14-3-3a reverts the effect of R18 on HopQ1 stability. Wild-type HopQ1 protein carrying a C-terminal Flag epitope was transiently expressed in *N. benthamiana* leaves. Crude protein extract was supplemented with R18 and increasing amounts of recombinant 14-3-3a-Strep II protein isolated from *E. coli*, as indicated. HopQ1 was detected by immunoblot analysis using specific primary antibodies. The level of 14-3-3a was monitored using Strep-Tactin AP conjugate. Equal protein loading was shown by Ponceau Red staining. (E) Assembled *in vitro* complex of HopQ1-6xHis and 14-3-3a-Strep II was incubated with bean crude protein extract in the absence or presence of the R18. HopQ1 and 14-3-3a were detected by immunoblot analyses using anti-His antibodies or Strep-Tactin AP conjugate, respectively. Equal protein loading was shown by Ponceau Red staining. (F) *In vitro* phosphorylated HopQ1-6xHis was added to bean crude extract and incubated in the presence of 14-3-3a or BSA. HopQ1 and 14-3-3a were detected by immunoblot analyses using anti-His antibodies or Strep-Tactin AP conjugate, respectively. Equal protein loading was shown by Ponceau Red staining.



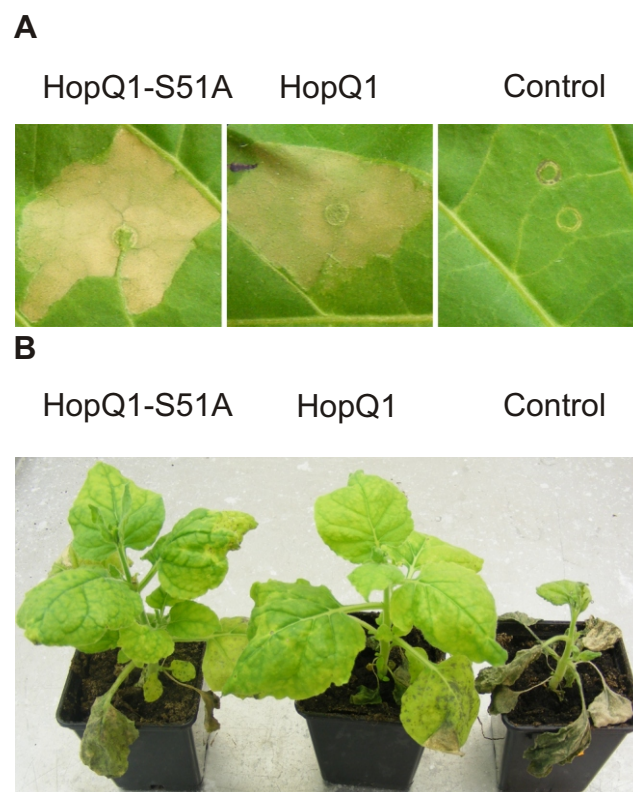


**Figure 8.** HopQ1 interaction with 14-3-3s is not critical for its perception by host plants. (A) Binary vectors encoding either wild-type HopQ1 or HopQ1-S51A were introduced via agroinfiltration into leaves of *Nicotiana tabacum*. Hypersensitive response developed in the infiltrated area within 48h, in response to both *Agrobacterium* strains. In contrast, no macroscopic signs of tissue necrotization developed in control leaves expressing GFP. (B) *Nicotiana benthamiana* plants were inoculated with *Pseudomonas syringae* pv. *syringae* B728a strains carrying pBBR1-MCS2 derivatives, which express either HopQ1, HopQ1-S51A or Cherry protein, as a control. Disease symptoms developed only in control plants treated with *P. syringae* pv. *syringae* B728a encoding Cherry protein. The pictures were taken 10 days post-inoculation. The experiments were performed three times with similar results.



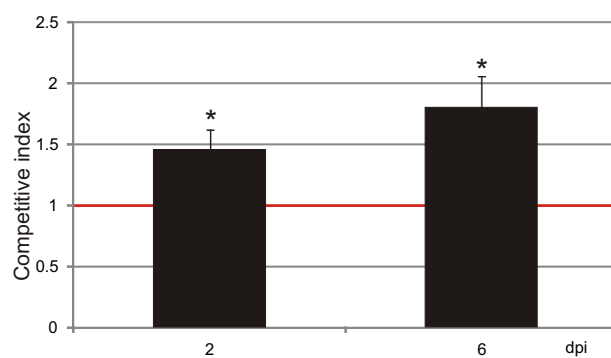


**Figure 9.** Assessment of virulence properties of HopQ1 effector mutated to eliminate 14-3-3 binding. Bean leaves were inoculated with *P. syringae* pv. *tomato* DC3000D28E ( $\sim 10^5$  CFU ml<sup>-1</sup>) strains expressing HopQ1 or HopQ1-S51A. Immediately prior to infiltration, bacteria were mixed in a 1:1 ratio. Two and six days post inoculation, two leaf discs per plant were cut out from the infiltrated zones, ground in sterile 10 mM MgCl<sub>2</sub>, diluted and plated on KB medium. Bacterial strains were distinguished by a selectable marker. The competitive index was calculated as the ratio of bacteria expressing the wild-type HopQ1 to bacteria expressing the mutated HopQ1 isolated from plant leaf and normalized to the input titers of the bacteria. Asterisks indicate that the index is significantly different from one, as established using Student's *t*-test ( $P=0.01$ ). The experiment was performed three times with similar results.